

# Domain walls in strontium titanate

**C. Stephen Hellberg**

U.S. Naval Research Laboratory, Washington, DC 20375, USA

E-mail: [steve.hellberg@nrl.navy.mil](mailto:steve.hellberg@nrl.navy.mil)

**Abstract.** Density functional theory calculations of twin-domain walls in strontium titanate are presented. The two possible domain walls are characterized. The domain wall type is set by the relative phase of the octahedral rotations in the body-centered-tetragonal SrTiO<sub>3</sub> on either side of the domain wall. The width of the domain walls is estimated to be approximately 3 nm.

## 1. Introduction

SrTiO<sub>3</sub> has the cubic perovskite crystal structure at room temperature. Below approximately 105 K, it undergoes a cubic to tetragonal structural transition [1, 2, 3, 4, 5, 6, 7, 8]. The oxygen octahedra rotate along one of the three crystallographic axes, and there is a slight elongation along that axis. The rotations alternate in each layer, making the crystal structure body-centered tetragonal [9, 10]. Twin-domain walls form between different tetragonal domains [11, 12, 13, 14].

At even lower temperatures, SrTiO<sub>3</sub> becomes a quantum paraelectric: ferroelectric ordering is suppressed by quantum fluctuations. When grown with a heavier isotope of oxygen, <sup>18</sup>O, SrTiO<sub>3</sub> becomes ferroelectric at 23 K [15]. With the much more common <sup>16</sup>O, SrTiO<sub>3</sub> is paraelectric, but with local ferroelectric regions [16]. Strain can be used to induce bulk ferroelectricity in SrTiO<sub>3</sub> by growing it on a substrate with a slightly different lattice constant [17, 18, 19, 20, 21, 22, 23, 24].

In recent years, growth of oxide heterostructures with atomic-scale precision has become possible [25, 26]. In particular, construction of interfaces with mismatched polarities, which is not possible in semiconductor heterostructures [27], was achieved in the LaAlO<sub>3</sub>/SrTiO<sub>3</sub> heterostructure [28, 29, 30].

LaAlO<sub>3</sub> and SrTiO<sub>3</sub> both have the same cubic perovskite crystal structure at room temperature, but in LaAlO<sub>3</sub> both cations have nominal charge +3, while Sr is +2 and Ti is +4. Both materials are conventional band insulators, and they are nearly lattice matched [31]. When grown in the [001] direction, each layer in SrTiO<sub>3</sub> is nominally charge neutral, while the layers in LaAlO<sub>3</sub> are alternatively positive and negative. The (001) surface can be prepared so that it is terminated by a TiO<sub>2</sub> layer [28]. The LaAlO<sub>3</sub> grown on this surface naturally forms a (largely) LaO layer on top of the TiO<sub>2</sub> layer [32] forming an *n*-type interface [30]. Once the LaAlO<sub>3</sub> film exceeds a critical thickness of close to four unit cells (approximately 1.6 nm), a conducting interface forms at the interface [29]. The carriers are electrons in the conduction band of the SrTiO<sub>3</sub> which are electrostatically bound to the interface.

At a thickness of approximately three unit cells, the nominally insulating interface can be made conducting locally by patterning the LaAlO<sub>3</sub> surface with a positively charged Atomic Force Microscope (AFM) tip [33]. The patterning is done at room temperature in humid air—it is believed that the AFM changes the surface charge locally by removing adsorbed OH<sup>-</sup> molecules

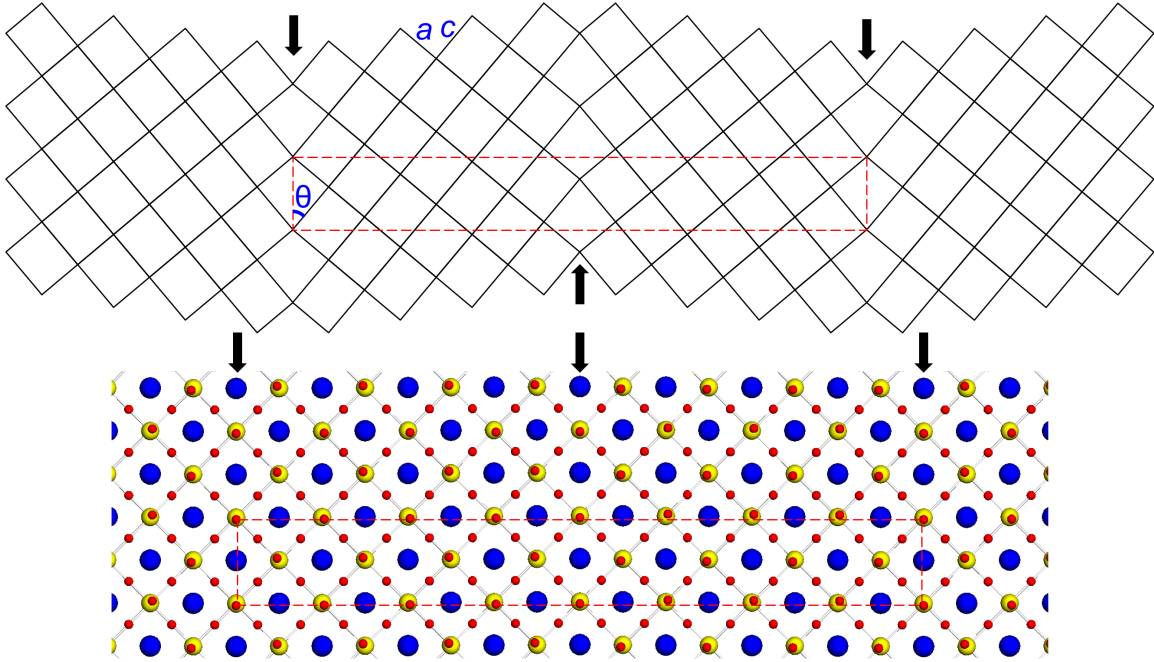


**Figure 1.** Top panel shows the schematic structure of the periodic computational cell containing two domain walls outlined by the dashed red rectangle. The  $c/a$  ratio is increased for clarity. Domain walls are indicated by the black arrows. The  $\hat{x}$  direction is into the page,  $\hat{y}$  is to the top of the page, and  $\hat{z}$  is to the right. The bottom panel shows the initial unrelaxed structure of a domain wall with  $N = 8$  (see the text). Sr atoms are blue, Ti are yellow, and oxygens are red. This supercell is too small to support domain walls, and the structure relaxes to a uniform phase.

[34]. Nanostructures with dimensions as small as 2 nm can be patterned in this manner [35]. This technique has been used to pattern quantum dots in  $\text{SrTiO}_3$  [36]. Tunneling through dots created in this manner showed that electrons pair in this system at temperatures several times the superconducting critical temperature in  $\text{SrTiO}_3$  [37]. In a separate experiment on wires of varying widths, it was found that the superconducting critical current is *independent* of the wire width, indicating that the superconducting transport is along the edges of the wires [38].

The surface patterning to create the wires dopes electrons into the  $\text{SrTiO}_3$  causing the  $\text{SrTiO}_3$  to expand by orienting the tetragonal domains normal to the surface [8]. If the tetragonal domains in the undoped regions neighboring the wires remains oriented in the plane, domain walls will be created between doped  $\hat{z}$ -domains under the wire and undoped  $\hat{x}$ - or  $\hat{y}$ -domains next to the wires [38]. Other experiments have shown enhanced conductivity along domain walls in  $\text{SrTiO}_3$  [39] and slightly increased superconducting  $T_c$  at domain walls [40]. Enhanced conductivity along domain walls has been observed in other materials, such as doped  $\text{WO}_3$  [41, 42, 43, 44], along grain boundaries in graphene [45, 46, 47], and in self organized stripes in the cuprates [48, 49]. Enhanced superconductivity has been observed in artificially layered metamaterials [50].

In this paper, we present Density Functional Theory (DFT) calculations of domain walls in  $\text{SrTiO}_3$  to examine their atomic structure and to determine the interactions between domain walls.

## 2. Computational details

The properties of SrTiO<sub>3</sub> and other perovskites depend sensitively on the choice of exchange-correlation functional [51]. We use the PBEsol functional, which has been shown to reproduce the lattice constants of SrTiO<sub>3</sub> very accurately [52, 53]. We use projector augmented wave functions as implemented in the Vienna *ab initio* simulation package (VASP) [54, 55, 56]. A plane wave cutoff of 283 eV and  $4 \times 4 \times 4$  Monkhorst-Pack  $k$ -points were used for the 20-atom tetragonal cell. A  $4 \times 4 \times 2$   $k$ -point mesh was used for the domain wall calculations. Atomic positions were relaxed until residual forces were less than 1 meV/Å. We find the optimal lattice constants of SrTiO<sub>3</sub> are  $a = 3.893$  Å and  $c = 3.922$  Å, yielding a  $c/a$  ratio of 1.0076.

Periodic computational cells are required for all calculations using VASP. We construct the supercell for the domain wall calculations as shown in Fig. 1. We rotate the tetragonal cell about the  $\hat{x}$ -axis by an angle  $\theta = \tan^{-1}(a/c)$ . We tile the rotated cell along its elongated direction, and reflect the structure about the  $xy$ -plane to create the other domain. The resulting translation vectors for the supercell are:

$$\begin{aligned} \mathbf{T}_1 &= 2a \hat{\mathbf{x}} \\ \mathbf{T}_2 &= \sqrt{a^2 + c^2} \hat{\mathbf{y}} \\ \mathbf{T}_3 &= 2N \frac{ac}{\sqrt{a^2 + c^2}} \hat{\mathbf{z}} \end{aligned} \quad (1)$$

for integer  $N$ , resulting in  $4N$  formula units in the supercell. Note that the length of  $\mathbf{T}_1$  must be an even multiple of  $a$  to accommodate the octahedral rotations; there is no similar restriction on  $\mathbf{T}_2$ .

## 3. Atomic structure of domain walls

Due to the rotation of the octahedra, two types of domain wall are possible as shown in Fig. 2. The first type has reflection symmetry about the domain wall; the second type is symmetric after a reflection plus a glide vector of  $\mathbf{G} = a \hat{\mathbf{x}}$ . The supercells for both domain walls have identical translation vectors.

We use the rotation axis of the oxygen octahedra as our order parameter. In both types of domain wall, the order parameter gently rotates through the domain wall [14]. With reflection symmetry, the order parameter rotates through the normal to the domain wall. With reflection-glide symmetry, the order parameter rotates through the plane of the domain wall. Notice that the type of domain wall is determined by the relative phases of the octahedral rotations in the tetragonal regions on either side of the domain wall. Thus the type of domain wall is robust and cannot be altered by shifting the domain wall or by creating local disorder.

## 4. Interactions between domain wall

To study the interactions between domain walls, we performed a series of calculations varying the distance between the domain walls by varying  $N$  in equation (1). To compute the formation energy for the domain walls, we need a reference energy, ideally of a pure tetragonal phase with the same number of formula units. However, tetragonal SrTiO<sub>3</sub> cannot have the same translation vectors as the domain wall calculations. We tried determining a reference energy from a calculation of the tetragonal structure with nearly the same translation vectors as those used for the domain walls.  $\mathbf{T}_1$  and  $\mathbf{T}_2$  are unchanged and  $\mathbf{T}_3$  is adjusted by the shortest possible shift to accommodate the tetragonal structure:

$$\Delta \mathbf{T}_3 = N \frac{c^2 - a^2}{\sqrt{a^2 + c^2}} \hat{\mathbf{y}}. \quad (2)$$

In this study,  $N \leq 32$ , and equation (2) is optimal; for significantly larger  $N$ , which would be computationally very expensive, equation (2) would no longer give the shortest shift consistent

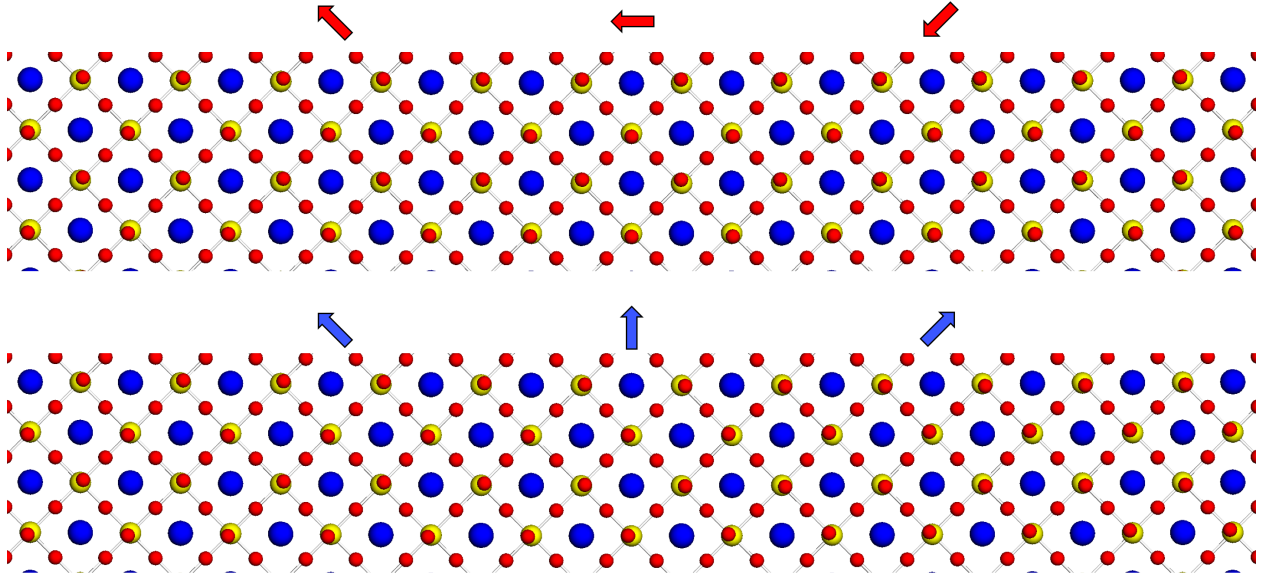


**Figure 2.** Relaxed structure of isolated domain walls with  $N = 32$ . Each structure has a domain wall in the center of the figure. The order parameter, the axis of rotation of the oxygen octahedra, is indicated by the arrows. The upper structure has reflection symmetry about the domain wall; the axis of octahedral rotation, indicated by the red arrows, rotates through the normal to the domain wall. The lower structure has glide-reflection symmetry, with a glide vector of  $\mathbf{G} = a \hat{x}$  (into the page); the axis of octahedral rotation, indicated by the blue arrows, rotates through the plane of the domain wall.

with a purely tetragonal structure. Unfortunately, the energy differences as a function of domain wall separation calculated in this manner were noisy, probably due to the different  $k$ -point sampling in the differently shaped computational cells.

Computing the energy difference between a supercell containing four and two domain walls allows exactly the same supercell to be used in both calculations. The results are shown in Fig. 3. In the limit of large separations, the two types of domain walls have comparable but clearly different energies. At distances less than 1 nm, the domain walls essentially annihilate, and the ions form a uniform phase, resulting in no energy difference between the calculations with four and two domain walls. These results show that interactions between domain walls in  $\text{SrTiO}_3$  does not extend beyond about 3nm.

## 5. Summary

Domain walls dominate the properties of many materials [44]. In  $\text{SrTiO}_3$  experiments indicate that domain walls likely play a critical role in superconducting transport. We computed the atomic structure of domain walls in  $\text{SrTiO}_3$  using density functional theory. Due to the body-centered-tetragonal structure of  $\text{SrTiO}_3$  at low temperatures, two types of domain walls are possible. We find the static interactions between domain walls are negligible beyond a distance of approximately 3 nm.

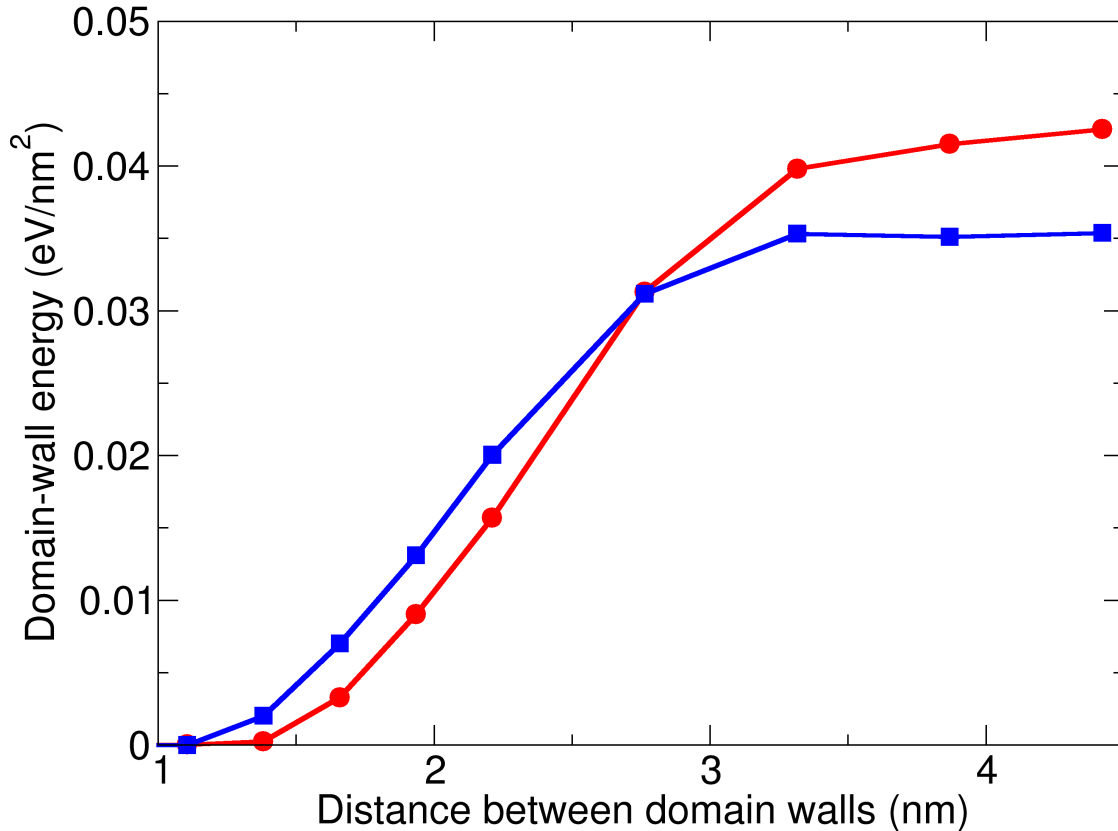


**Figure 3.** Energy of domain walls as a function of their separation. The domain-wall energy is computed from the energy difference between identical supercells containing four and two domain walls. The distance is defined as 25% of the long axis of the supercell. Domain walls with reflection symmetry are plotted as red circles; domain walls with glide-reflection symmetry are blue squares.

### Acknowledgments

Insightful discussions with Jeremy Levy, Massimiliano Stengel, Johnathan Ruhman, Patrick A. Lee, and Madeleine Phillips are gratefully acknowledged. This work was supported by the Office of the Secretary of Defense through the LUCI program and by a grant of computer time from the DoD High Performance Computing Modernization Program.

### References

- [1] Lytle, F. W. X-Ray Diffractometry of Low-Temperature Phase Transformations in Strontium Titanate. *Journal Of Applied Physics* **35**, 2212–2215 (1964).
- [2] Sai, N. and Vanderbilt, D. First-principles study of ferroelectric and antiferrodistortive instabilities in tetragonal SrTiO<sub>3</sub>. *Physical Review B* **62**, 13942–13950 (2000).
- [3] Howard, C. J. and Stokes, H. T. Structures and phase transitions in perovskites – a group-theoretical approach. *Acta Crystallographica Section A: Foundations of Crystallography* **61**, 93–111 (2005).
- [4] Zubko, P., Catalan, G., Buckley, A., Welche, P. R. L., and Scott, J. F. Strain-Gradient-Induced Polarization in SrTiO<sub>3</sub> Single Crystals. *Physical Review Letters* **99**, 167601 (2007).

- [5] Evarestov, R. A., Blokhin, E., Gryaznov, D., Kotomin, E. A., and Maier, J. Phonon calculations in cubic and tetragonal phases of SrTiO<sub>3</sub>: A comparative LCAO and plane-wave study. *Physical Review B* **83**, 134108 (2011).
- [6] Scott, J., Salje, E., and Carpenter, M. Domain Wall Damping and Elastic Softening in SrTiO<sub>3</sub>: Evidence for Polar Twin Walls. *Physical Review Letters* **109**, 187601 (2012).
- [7] Morozovska, A. N., Eliseev, E. A., Glinchuk, M. D., Chen, L.-Q., and Gopalan, V. Interfacial polarization and pyroelectricity in antiferrodistortive structures induced by a flexoelectric effect and rotostriction. *Physical Review B* **85**, 094107 (2012).
- [8] Honig, M., Sulpizio, J. A., Drori, J., Joshua, A., Zeldov, E., and Ilani, S. Local electrostatic imaging of striped domain order in LaAlO<sub>3</sub>/SrTiO<sub>3</sub>. *Nature Materials* **12**, 1112–1118 (2013).
- [9] Setyawan, W. and Curtarolo, S. High-throughput electronic band structure calculations: Challenges and tools. *Computational Materials Science* **49**, 299–312 (2010).
- [10] Mehl, M. J., Hicks, D., Toher, C., Levy, O., Hanson, R. M., Hart, G., and Curtarolo, S. The AFLOW Library of Crystallographic Prototypes: Part 1. *Computational Materials Science* **136**, S1–S828 (2017).
- [11] Tagantsev, A. K., Courtens, E., and Arzel, L. Prediction of a low-temperature ferroelectric instability in antiphase domain boundaries of strontium titanate. *Physical Review B* **64**, 224107 (2001).
- [12] Merz, T. A., Noad, H., Xu, R., Inoue, H., Liu, W., Hikita, Y., Vailionis, A., Moler, K. A., and Hwang, H. Y. Depth resolved domain mapping in tetragonal SrTiO<sub>3</sub> by micro-Laue diffraction. *Applied Physics Letters* **108**, 182901 (2016).
- [13] Gray, Jr, D. J., Merz, T. A., Hikita, Y., Hwang, H. Y., and Mabuchi, H. Orientation-resolved domain mapping in tetragonal SrTiO<sub>3</sub> using polarized Raman spectroscopy. *Physical Review B* **94**, 214107 (2016).
- [14] Schiaffino, A. and Stengel, M. Macroscopic Polarization from Antiferrodistortive Cycloids in Ferroelastic SrTiO<sub>3</sub>. *Physical Review Letters* **119**, 137601 (2017).
- [15] Itoh, M., Wang, R., Inaguma, Y., Yamaguchi, T., Shan, Y.-J., and Nakamura, T. Ferroelectricity Induced by Oxygen Isotope Exchange in Strontium Titanate Perovskite. *Physical Review Letters* **82**, 3540–3543 (1999).
- [16] Tikhomirov, O., Jiang, H., and Levy, J. Local Ferroelectricity in SrTiO<sub>3</sub> Thin Films. *Physical Review Letters* **89**, 147601 (2002).
- [17] Pertsev, N. A., Tagantsev, A. K., and Setter, N. Phase transitions and strain-induced ferroelectricity in SrTiO<sub>3</sub> epitaxial thin films. *Physical Review B* **61**, R825–R829 (2000).
- [18] Aguirre-Tostado, F. S., Herrera-Gómez, A., Woicik, J. C., Droopad, R., Yu, Z., Schlom, D. G., Zschack, P., Karapetrova, E., Pianetta, P., and Hellberg, C. S. Elastic anomaly for SrTiO<sub>3</sub> thin films grown on Si(001). *Physical Review B* **70**, 201403 (2004).
- [19] Haeni, J. H., Irvin, P., Chang, W., Uecker, R., Reiche, P., Li, Y. L., Choudhury, S., Tian, W., Hawley, M. E., Craigo, B., Tagantsev, A. K., Pan, X. Q., Streiffer, S. K., Chen, L. Q., Kirchoefer, S. W., Levy, J., and Schlom, D. G. Room-temperature ferroelectricity in strained SrTiO<sub>3</sub>. *Nature* **430**, 758–761 (2004).
- [20] Woicik, J. C., Li, H., Zschack, P., Karapetrova, E., Ryan, P., Ashman, C. R., and Hellberg, C. S. Anomalous lattice expansion of coherently strained SrTiO<sub>3</sub> thin films grown on Si(001) by kinetically controlled sequential deposition. *Physical Review B* **73**, 024112 (2006).
- [21] Woicik, J. C., Shirley, E. L., Hellberg, C. S., Andersen, K. E., Sambasivan, S., Fischer, D. A., Chapman, B. D., Stern, E. A., Ryan, P., Ederer, D. L., and Li, H. Ferroelectric distortion in SrTiO<sub>3</sub> thin films on Si(001) by x-ray absorption fine structure spectroscopy: Experiment and first-principles calculations. *Physical Review B* **75**, 140103 (2007).
- [22] Kourkoutis, L. F., Hellberg, C. S., Vaithyanathan, V., Li, H., Parker, M. K., Andersen, K. E., Schlom, D. G., and Muller, D. A. Imaging the phase separation in atomically thin buried SrTiO<sub>3</sub> layers by electron channeling. *Physical Review Letters* **100** (2008).
- [23] Warusawithana, M. P., Cen, C., Sleasman, C. R., Woicik, J. C., Li, Y., Kourkoutis, L. F., Klug, J. A., Li, H., Ryan, P., Wang, L.-P., Bedzyk, M., Muller, D. A., Chen, L.-Q., Levy, J., and Schlom, D. G. A Ferroelectric Oxide Made Directly on Silicon. *Science* **324**, 367–370 (2009).
- [24] Hellberg, C. S., Andersen, K. E., Li, H., Ryan, P. J., and Woicik, J. C. Structure of SrTiO<sub>3</sub> Films on Si. *Physical Review Letters* **108**, 166101 (2012).
- [25] Ohtomo, A., Muller, D. A., Grazul, J. L., and Hwang, H. Y. Artificial charge-modulation in atomic-scale perovskite titanate superlattices. *Nature* **419**, 378–380 (2002).
- [26] Muller, D. A., Nakagawa, N., Ohtomo, A., Grazul, J. L., and Hwang, H. Y. Atomic-scale imaging of nanoengineered oxygen vacancy profiles in SrTiO<sub>3</sub>. *Nature* **430**, 657–661 (2004).
- [27] Harrison, W. A., Kraut, E. A., Waldrop, J. R., and Grant, R. W. Polar heterojunction interfaces. *Physical Review B* **18**, 4402–4410 (1978).
- [28] Ohtomo, A. and Hwang, H. Y. A high-mobility electron gas at the LaAlO<sub>3</sub>/SrTiO<sub>3</sub> heterointerface. *Nature* **427**, 423–426 (2004).

- [29] Thiel, S., Hammerl, G., Schmehl, A., Schneider, C. W., and Mannhart, J. Tunable Quasi-Two-Dimensional Electron Gases in Oxide Heterostructures. *Science* **313**, 1942–1945 (2006).
- [30] Nakagawa, N., Hwang, H. Y., and Muller, D. A. Why some interfaces cannot be sharp. *Nature Materials* **5**, 204–209 (2006).
- [31] Pai, Y.-Y., Tylan-Tyler, A., Irvin, P., and Levy, J. Physics of SrTiO<sub>3</sub>-based heterostructures and nanostructures: a review. *Reports On Progress In Physics* **81**, 036503 (2018).
- [32] Warusawithana, M. P., Richter, C., Mundy, J. A., Roy, P., Ludwig, J., Paetel, S., Heeg, T., Pawlicki, A. A., Kourkoutis, L. F., Zheng, M., Lee, M., Mulcahy, B., Zander, W., Zhu, Y., Schubert, J., Eckstein, J. N., Muller, D. A., Hellberg, C. S., Mannhart, J., and Schlom, D. G. LaAlO<sub>3</sub> stoichiometry is key to electron liquid formation at LaAlO<sub>3</sub>/SrTiO<sub>3</sub> interfaces. *Nature Communications* **4**, 2351 (2013).
- [33] Cen, C., Thiel, S., Hammerl, G., Schneider, C. W., Andersen, K. E., Hellberg, C. S., Mannhart, J., and Levy, J. Nanoscale control of an interfacial metal-insulator transition at room temperature. *Nature Materials* **7**, 298–302 (2008).
- [34] Bi, F., Bogorin, D. F., Cen, C., Bark, C. W., Park, J.-W., Eom, C.-B., and Levy, J. “Water-cycle” mechanism for writing and erasing nanostructures at the LaAlO<sub>3</sub>/SrTiO<sub>3</sub> interface. *Applied Physics Letters* **97**, 173110 (2010).
- [35] Cen, C., Thiel, S., Mannhart, J., and Levy, J. Oxide Nanoelectronics on Demand. *Science* **323**, 1026–1030 (2009).
- [36] Cheng, G., Tomczyk, M., Lu, S., Veazey, J. P., Huang, M., Irvin, P., Ryu, S., Lee, H., Eom, C.-B., Hellberg, C. S., and Levy, J. Electron pairing without superconductivity. *Nature* **521**, 196–199 (2015).
- [37] Eagles, D. Possible Pairing without Superconductivity at Low Carrier Concentrations in Bulk and Thin-Film Superconducting Semiconductors. *Physical Review* **186**, 456–463 (1969).
- [38] Pai, Y.-Y., Lee, H., Lee, J.-W., Annadi, A., Cheng, G., Lu, S., Tomczyk, M., Huang, M., Eom, C.-B., Irvin, P., and Levy, J. One-Dimensional Nature of Pairing and Superconductivity at the LaAlO<sub>3</sub>/SrTiO<sub>3</sub> Interface. *Preprint at <https://arxiv.org/abs/1707.01468>* (2017).
- [39] Kalisky, B., Spanton, E. M., Noad, H., Kirtley, J. R., Nowack, K. C., Bell, C., Sato, H. K., Hosoda, M., Xie, Y., Hikita, Y., Woltmann, C., Pfanzelt, G., Jany, R., Richter, C., Hwang, H. Y., Mannhart, J., and Moler, K. A. Locally enhanced conductivity due to the tetragonal domain structure in LaAlO<sub>3</sub>/SrTiO<sub>3</sub> heterointerfaces. *Nature Materials* **12**, 1091–1095 (2013).
- [40] Noad, H., Spanton, E. M., Nowack, K. C., Inoue, H., Kim, M., Merz, T. A., Bell, C., Hikita, Y., Xu, R., Liu, W., Vaillonis, A., Hwang, H. Y., and Moler, K. A. Variation in superconducting transition temperature due to tetragonal domains in two-dimensionally doped SrTiO<sub>3</sub>. *Physical Review B* **94**, 174516 (2016).
- [41] Aird, A. and Salje, E. K. H. Sheet superconductivity in twin walls: experimental evidence of WO<sub>3-x</sub>. *J. Phys. Condens. Matter* **10**, L377–L380 (1998).
- [42] Aird, A., Domeneghetti, M. C., Mazzi, F., Tazzoli, V., and Salje, E. K. H. Sheet superconductivity in WO<sub>3-x</sub>: crystal structure of the tetragonal matrix. *J. Phys. Condens. Matter* **10**, L569–L574 (1998).
- [43] Kim, Y., Alexe, M., and Salje, E. K. H. Nanoscale properties of thin twin walls and surface layers in piezoelectric WO<sub>3-x</sub>. *Applied Physics Letters* **96**, 032904 (2010).
- [44] Catalan, G., Seidel, J., Ramesh, R., and Scott, J. F. Domain wall nanoelectronics. *Reviews of Modern Physics* **84**, 119–156 (2012).
- [45] Lahiri, J., Lin, Y., Bozkurt, P., Oleynik, I. I., and Batzill, M. An extended defect in graphene as a metallic wire. *Nature Nanotechnology* **5**, 326–329 (2010).
- [46] Phillips, M. and Mele, E. J. Zero modes on zero-angle grain boundaries in graphene. *Physical Review B* **91**, 125404 (2015).
- [47] Phillips, M. and Mele, E. J. Charge and spin transport on graphene grain boundaries in a quantizing magnetic field. *Physical Review B* **96**, 041403 (2017).
- [48] Hellberg, C. S. and Manousakis, E. Stripes and the *t*-*J* Model. *Physical Review Letters* **83**, 132–135 (1999).
- [49] Rajasekaran, S., Okamoto, J., Mathey, L., Fechner, M., Thampy, V., Gu, G. D., and Cavalleri, A. Probing optically silent superfluid stripes in cuprates. *Science (New York, NY)* **359**, 575–579 (2018).
- [50] Smolyaninova, V. N., Jensen, C., Zimmerman, W., Prestigiacomo, J. C., Osofsky, M. S., Kim, H., Bassim, N., Xing, Z., Qazilbash, M. M., and Smolyaninov, I. I. Enhanced superconductivity in aluminum-based hyperbolic metamaterials. *Scientific Reports* **6**, 34140 (2016).
- [51] Gebhardt, J. and Rappe, A. M. Accuracy and Transferability of *Ab Initio* Electronic Band Structure Calculations for Doped BiFeO<sub>3</sub>. *Journal of Physics: Conference Series* **921**, 012009 (2017).
- [52] Perdew, J. P., Ruzsinszky, A., Csonka, G. I., Vydrov, O. A., Scuseria, G. E., Constantin, L. A., Zhou, X., and Burke, K. Restoring the Density-Gradient Expansion for Exchange in Solids and Surfaces. *Physical Review Letters* **100**, 136406 (2008).
- [53] Aschauer, U. and Spaldin, N. A. Competition and cooperation between antiferrodistortive and ferroelectric instabilities in the model perovskite SrTiO<sub>3</sub>. *J. Phys. Condens. Matter* **26**, 122203 (2014).

- [54] Kresse, G. and Furthmüller, J. Efficient iterative schemes for ab initio total-energy calculations using a plane-wave basis set. *Physical Review B* **54**, 11169–11186 (1996).
- [55] Kresse, G. and Joubert, D. From ultrasoft pseudopotentials to the projector augmented-wave method. *Physical Review B* **59**, 1758–1775 (1999).
- [56] Blöchl, P. E. Projector augmented-wave method. *Physical Review B* **50**, 17953–17979 (1994).